

Origin of Enantioselective Hydrogenation of Ketones by RuH₂(diphosphine)(diamine) Catalysts: A Theoretical Study

Tom Leyssens,[†] Daniel Peeters,[†] and Jeremy N. Harvey^{*‡‡}

Laboratoire de Chimie Quantique, Université Catholique de Louvain, Place Louis Pasteur 1, B-1348 Louvain-la-Neuve, Belgium, and School of Chemistry, University of Bristol, Cantock's Close, Bristol BS8 1TS, U.K.

Received September 21, 2007

The origin of the enantioselective hydrogenation of acetophenone by the (*S*-BINAP)RuH₂(*S,S*-cydn) (cydn = 1,2-cyclohexanediamine) catalyst has been investigated by a theoretical DFT study. Computations for hydrogenation of acetone and acetophenone by the model system RuH₂(PH₃)₂(en) (en = 1,2 ethylenediamine) confirm the previously proposed mechanism. These calculations show that reaction involving two of the four NH protons, which adopt a pseudoaxial orientation in the catalyst, is favored by ca. 2 kcal/mol over reaction involving the other two pseudoequatorial protons. The results for the model system reacting with acetophenone show that approach of the ketone with the phenyl group oriented away from the phosphine ligands (“out” approach) is favored by weak hydrogen bonding between the ketone phenyl group and one of the ruthenium-coordinated NH₂ groups. In the full (*S*-BINAP)RuH₂(*S,S*-cydn) catalyst, steric interactions also contribute to establishing the *R* selectivity in hydrogenation, and the magnitude of this selectivity is reproduced semiquantitatively. Study of the mismatched (*S*-BINAP)RuH₂(*R,R*-cydn) also semiquantitatively reproduces the much reduced *R* selectivity of this catalyst and contributes to rationalizing it. Transfer of the less favored pseudoequatorial NH₂ proton plays a key role in this case. It is shown that the results can also be used to discuss selectivity in other related systems.

Introduction

Enantioselective hydrogenation of prochiral ketones to optically active alcohols is of crucial importance in synthetic chemistry. Very active catalysts for this reaction can be generated from the *trans* RuCl₂(diphosphine)(diamine) complexes, as developed for this purpose by Noyori and co-workers.^{1–8} Very high chemoselectivity is obtained with these systems for hydrogenation of the ketone group in the presence of other unsaturated functionalities (e.g., C=C double bonds), although it is also possible to reduce imines. The hydrogen source can be either an alcohol (transfer hydrogenation) or molecular hydrogen. The active catalysts have been shown to be the *trans* dihydride RuH₂(diphosphine)(diamine) species,^{9–11} generated from the dichloride precatalysts in the presence of a strong base¹² or directly from the hydrido-BH₄ complex under base-free conditions.¹³ The diamine ligand plays a crucial role in the activity of the catalyst. Indeed, the rapid hydrogenation is

believed to occur by a mechanism involving at the same time the metal center and the amine ligand, referred to as “metal–ligand difunctional catalysis” by Noyori.⁸ Related hydride–proton transfer reactions have been developed with other metal catalyst systems.

The likely catalytic cycle, proposed on the basis of experimental^{9,14–16} as well as computational^{16–19} observations, consists in two key steps (Scheme 1). First, concerted transfer of a metal-bound hydride to the carbonyl carbon atom and of an NH proton to the oxygen atom leads to the alcohol product and a RuH(diphosphine)(amido-amino) intermediate. In asymmetric catalysis, this step determines the enantioselectivity of the obtained alcohol. The active dihydride catalyst is regenerated

* Corresponding author. E-mail: Jeremy.Harvey@bristol.ac.uk.

[†] Université Catholique de Louvain.

^{‡‡} University of Bristol.

(1) Ohkuma, T.; Ooka, H.; Hashiguchi, S.; Ikariya, T.; Noyori, R. *J. Am. Chem. Soc.* **1995**, *117*, 2675–2676.

(2) Ohkuma, T.; Ooka, H.; Ikariya, T.; Noyori, R. *J. Am. Chem. Soc.* **1995**, *117*, 10417–10418.

(3) Noyori, R.; Hashiguchi, S. *Acc. Chem. Res.* **1997**, *30*, 97–102.

(4) Ohkuma, T.; Doucet, H.; Pham, T.; Mikami, K.; Korenaga, T.; Terada, M.; Noyori, R. *J. Am. Chem. Soc.* **1998**, *120*, 1086–1087.

(5) Ohkuma, T.; Koizumi, M.; Doucet, H.; Pham, T.; Kozawa, M.; Murata, K.; Katayama, E.; Yokozawa, T.; Ikariya, T.; Noyori, R. *J. Am. Chem. Soc.* **1998**, *120*, 13529–13530.

(6) Doucet, H.; Ohkuma, T.; Murata, K.; Yokozawa, T.; Kozawa, M.; Katayama, E.; England, F. E.; Ikariya, T.; Noyori, R. *Angew. Chem., Int. Ed.* **1998**, *37*, 1703–1707.

(7) Mikami, K.; Korenaga, T.; Terada, M.; Ohkuma, T.; Pham, T.; Noyori, R. *Angew. Chem., Int. Ed.* **1999**, *38*, 495–497.

(8) Noyori, R.; Ohkuma, T. *Angew. Chem., Int. Ed.* **2001**, *40*, 40–73.

(9) Abdur-Rashid, K.; Lough, A. J.; Morris, R. H. *Organometallics* **2000**, *19*, 2655–2657.

(10) Haack, K. J.; Hashiguchi, S.; Fujii, A.; Ikariya, T.; Noyori, R. *Angew. Chem., Int. Ed. Engl.* **1997**, *36*, 285–288.

(11) Abdur-Rashid, K.; Lough, A. J.; Morris, R. H. *Organometallics* **2001**, *20*, 1047–1049.

(12) Cappellani, E. P.; Maltby, P. A.; Morris, R. H.; Schweitzer, T. C.; Steele, M. R. *Inorg. Chem.* **1989**, *28*, 4437–4438.

(13) (a) Ohkuma, T.; Koizumi, M.; Muñoz, K.; Hilt, G.; Kabuto, C.; Noyori, R. *J. Am. Chem. Soc.* **2002**, *124*, 6508–6509. (b) Sandoval, C. A.; Yamaguchi, Y.; Ohkuma, T.; Kato, K.; Noyori, R. *Magn. Reson. Chem.* **2006**, *44*, 66–75.

(14) Abdur-Rashid, K.; Faatz, M.; Lough, A. J.; Morris, R. H. *J. Am. Chem. Soc.* **2001**, *123*, 7473–7474.

(15) Noyori, R.; Yamakawa, M.; Hashiguchi, S. *J. Org. Chem.* **2001**, *66*, 7931–7944.

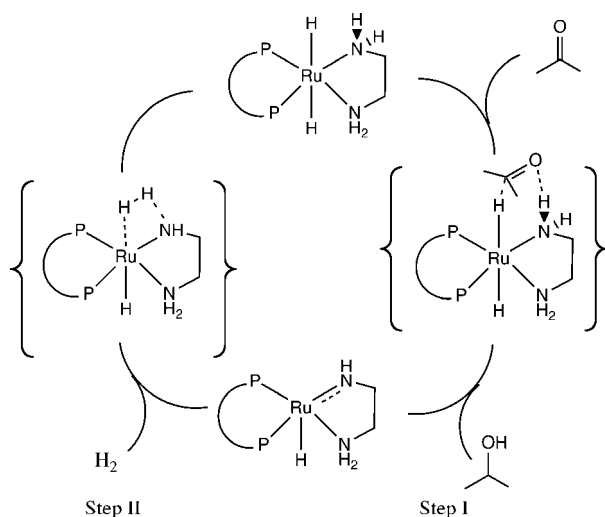
(16) Abdur-Rashid, K.; Clapham, S. E.; Hadzovic, A.; Harvey, J. N.; Lough, A. J.; Morris, R. H. *J. Am. Chem. Soc.* **2002**, *124*, 15104–15118.

(17) Alonso, D.; Brandt, P.; Nordin, S. J.; Andersson, P. G. *J. Am. Chem. Soc.* **1999**, *121*, 9580–9588.

(18) Yamakawa, M.; Ito, H.; Noyori, R. *J. Am. Chem. Soc.* **2000**, *122*, 1466–1478.

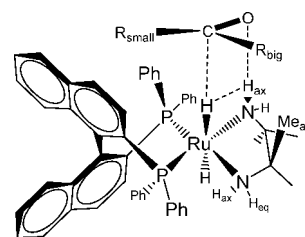
(19) Petra, D. G. I.; Reek, J. N. H.; Handgraaf, J. W.; Meijer, E. J.; Dierkes, P.; Kamer, P. C. J.; Brussee, J.; Schoemaker, H. E.; van Leeuwen, P. W. N. M. *Chem.–Eur. J.* **2000**, *6*, 2818–2829.

Scheme 1



in a second, rate-limiting,¹⁶ step through heterolytic splitting of dihydrogen across the formal Ru=N bond. An alternative catalytic cycle has been suggested to occur in parallel with the one described here under more acidic conditions.^{20,21} The first step in this other mechanism, hydrogenation of the ketone, is the same as in Scheme 1, but the path followed to regenerate the dihydride species is slightly different. The role of the base continues to attract attention, as it may react with some of the species in the active cycle as well as activating the precatalyst.²² As shown in Scheme 1, the catalytically most active isomer of the dihydride species is usually the one with a *trans* arrangement of the two hydrides, with the diphosphine and diamine lying in the same plane. However, other isomers exist, and in some cases, interconversion of the different isomers can occur at the same time as catalysis.²³

High enantioselectivities can be obtained in hydrogenation of prochiral ketones when using chiral amines or phosphines, or combinations of chiral amines and phosphines.⁸ Although the reaction is highly general, it is found that the best enantioselectivities sometimes require different chiral ligands for different substrates, and new chiral phosphines and amines continue to be tested and developed.^{24,25} To assist in the development of the catalyst, it is useful to understand the reaction mechanism and the origin of stereoselectivity, in detail. Based on experimental observations, a number of models have been proposed to account for the observed selectivity.^{14,20,21} For example, with C_2 -symmetric RuH_2 (BINAP)(diamine) catalysts, the ketone substrate has been proposed to prefer a mode of approach in which the more bulky of the two groups on the carbonyl carbon is oriented away from the naphthalene ring of the BINAP ligand. This proposed structure for the hydrogenation TS is shown in Chart 1 for the example of the *trans*- RuH_2 (BINAP)(tmen) complex¹⁴ (tmen = 1,2,3,4-tetramethyl-

Chart 1. Stereochemical Model Used to Explain the Enantioselectivity of the Dihydrogen Transfer from *trans*- RuH_2 -(BINAP)(tmen) to the Ketone

1,2-ethylenediamine). As shown in the chart, the chelating diamine ligand forms a five-membered ring in which the N-H hydrogens adopt either pseudoaxial (“H_{ax}”) or pseudoequatorial (“H_{eq}”) positions. The axial hydrogens are much better oriented for proton transfer to the substrate; hence reactivity has usually been assumed to occur predominantly from these hydrogens, although it has been mentioned that transfer of H_{eq} might contribute in some cases.^{18,20}

The steric model presented above successfully explains the high enantioselectivity (97% enantiomeric excess, or ee, for the *R* alcohol) obtained¹ in hydrogenation of 1'-acetonaftone using $RuCl_2$ (*S*-BINAP)(*S,S*-dpn) (dpn = 1,2-diphenylethylenediamine). It also accounts for the high ee of 91% *S* obtained in the similar reaction of 1'-acetonaftone with $RuCl_2$ (*R*-tolbinap)(*R,R*-dpn).⁶ Acetophenone gives a slightly lower ee of 80%.⁶ When using the other two possible combinations of bisphosphine and diamine chirality, namely, $RuCl_2$ (*S*-BINAP)(*R,R*-dpn) and $RuCl_2$ (*R*-tolbinap)(*S,S*-dpn), much lower ee's of 14% and 15% are obtained in favor of the *R* and *S* enantiomers, respectively.^{1,6} These results show that the dominant influence on the enantioselectivity is exerted by the bisphosphine ligand used, as the *S* isomer leads to preferential formation of the *R* alcohol, and vice versa. However, the much lower ee's observed with the “mismatch” *S,RR* and *R,SS* systems as compared to those obtained with the “matched” *S,SS* and *R,RR* catalysts show that the chirality of the diamine also plays an important role. The origin of this influence of the diamine chirality is not clear based on the steric model of Chart 1, which places the emphasis on the steric influence of the BINAP ligand.

To clarify this issue, we use computation in this paper to examine the origin of stereoselectivity in the catalytic cycle. Our calculations use two different models. First, we consider the hydrogenation reactions of a simple, nonprochiral ketone, acetone, and of a typical prochiral ketone, acetophenone, with the model RuH_2 (PH_3)₂(en) catalyst. These first calculations are a direct extension of our previous work on the same model¹⁶ and provide insight into the intrinsic reactivity of the system. Next, we will examine the catalytic cycle for the hydrogenation of acetophenone by the “real” RuH_2 (BINAP)(cydn) catalyst (cydn = *trans*-1,2-diaminocyclohexane). Experimentally, this gives enantioselectivities similar to those obtained with the complex with the dpn ligand mentioned above,⁵ and the geometry close to the ruthenium center is very similar. However, it is more convenient for computational study, as it involves slightly fewer atoms and is more conformationally rigid. In our calculations, we will consider both the matched *R,RR* and mismatched *R,SS* systems.

(20) Sandoval, C. A.; Ohkuma, T.; Muniz, K.; Noyori, R. *J. Am. Chem. Soc.* **2003**, *125*, 13490–13503.

(21) Clapham, S. E.; Hadzovic, A.; Morris, R. H. *Coord. Chem. Rev.* **2004**, *248*, 2201–2237.

(22) See for example: Hamilton, R. J.; Bergens, S. H. *J. Am. Chem. Soc.* **2006**, *128*, 13700–13701.

(23) Abbel, R.; Abdur-Rashid, K.; Faatz, M.; Hadzovic, A.; Lough, A. J.; Morris, R. H. *J. Am. Chem. Soc.* **2005**, *127*, 1870–1882.

(24) (a) See for example: Ohkuma, T.; Sandoval, C. A.; Srinivasan, R.; Lin, Q.; Wei, Y.; Muñiz, K.; Noyori, R. *J. Am. Chem. Soc.* **2005**, *117*, 8288–8289. (b) Xu, Y.; Docherty, G. F.; Woodward, G.; Wills, M. *Tetrahedron: Asymmetry* **2006**, *17*, 2925–2929.

(25) Hems, W. P.; Groarke, M.; Zanotti-Gerosa, A.; Grasa, G. A. *Acc. Chem. Res.* **2007**, *40*, 1340.

Computational Details

All structures were fully optimized using Becke's three-parameter hybrid functional (B3LYP), as implemented in the Jaguar²⁶ and Gaussian 03²⁷ series of programs. Optimized geometries are provided in the Supporting Information. Frequency calculations were carried out using Gaussian²⁷ at stationary points, so as to derive a correction for zero-point energy. For transition states, a single imaginary frequency was obtained, and the corresponding normal mode was inspected to check that the correct TS had been located. In both Gaussian and Jaguar calculations, the Ru atom was described using an effective core potential to represent all but the valence nd and $(n + 1)s$ and outer core ns and np electrons.²⁸ The latter were described with a triple- ζ contraction of the original double- ζ basis set; this combination is referred to as the LACV3P basis set.²⁶ For the $\text{RuH}_2(\text{PH}_3)_2(\text{en})$ system, all nonmetal atoms were described using the standard 6-31G** basis set (with only the five spherical harmonic d functions). For the more complex $\text{RuH}_2(\text{BINAP})(\text{cydn})$ system, all nonmetal atoms have been treated with a 6-31G basis set with the exception of the P and N atoms, of the H atoms linked to Ru and N, and of the atoms of the acetophenone molecule, which have been treated with a 6-31G** basis set. Unless mentioned otherwise, all geometries and energies mentioned below were obtained with this combination of basis sets, referred to in short as the 6-31G* basis set. Atomic charges were calculated using the NBO method.²⁹

Additional single-point energy calculations were performed in some cases at the B3LYP geometries at the MP2 level of theory, using the same 6-31G* basis set. It has been shown that for many systems, scaling of the different spin-state components of the MP2 correlation energy can lead to more accurate results.^{30,31} Accordingly, we have applied this spin-component scaling and hence report "SCS-MP2" energies. Single-point energies have also been computed at the B3LYP level of theory using an expanded basis set. For ruthenium, this used the Stuttgart–Dresden ECP with the associated triple- ζ basis, to which two f polarization functions were added ($\zeta = 1.666$ and 0.478). On all other atoms, the standard 6-311G** basis was used. This combination is referred to in short as the 6-311G** basis. These single-point energies were derived using the Gaussian program.²⁷ All quoted energies include a correction for zero-point energy derived at the B3LYP level using the 6-31G* basis set.

Results and Discussion

A. Reaction of Acetone and Acetophenone with the Model System.

Our initial calculations were designed to probe the potential energy surface for the whole catalytic cycle for

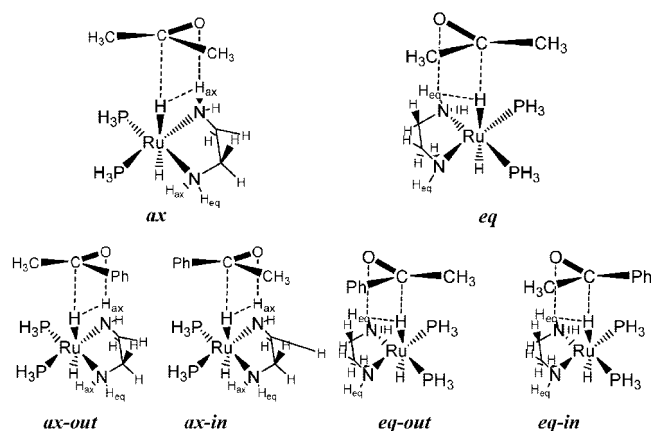


Figure 1. Possible approaches of acetone and acetophenone with respect to the $\text{RuH}_2((\text{PH}_3)_2(\text{en}))$ catalyst.

Table 1. B3LYP/6-31G* Energies (kcal/mol) Relative to Reactants for the Species in the Catalytic Cycles for Hydrogenation of Acetone or Acetophenone by the $\text{RuH}_2(\text{PH}_3)_2(\text{en})$ Model Catalyst (species labels refer to Figure 2)^a

	acetone		acetophenone			
	ax	eq	ax-out	ax-in	eq-out	eq-in
A	0.00 (0.00 , 0.00)	0.00	0.00	0.00	0.00	0.00
B	-7.29 (-5.26 , -6.69)	-6.73	-6.38	-6.07	-5.91	-5.95
C	-3.41 (0.05 , -2.44)	-1.50	-3.20	-2.77	-2.10	-1.01
D	-11.91 (-9.54 , -10.58)	-9.49	-11.24	-10.91	-10.33	-8.17
E	-2.51 (-2.12 , -3.59)	-0.46	-0.67	-0.67	1.38	1.38
F	2.34 (2.47 , 0.44)	2.22	4.18	4.18	4.05	4.05
G	11.79 (15.36 , 10.74)	13.78	13.62	13.62	15.61	15.61
H	-7.30 (-8.43 , -7.24)	-7.30	-5.46	-5.46	-5.46	-5.46

^a Single-point energies at the SCS-MP2^{30,31}/6-31G* (in bold) and B3LYP/6-311G** (in italics) levels of theory are shown in parentheses for the reaction with acetone with the axial approach.

hydrogenation by the model $\text{RuH}_2(\text{PH}_3)_2(\text{en})$ catalyst. These calculations also allow us to explore whether there is an intrinsic difference in reactivity between the axial and equatorial hydrogens on the diamine ligand and between the Re and Si faces of acetophenone for a given approach to the catalyst. In this case, the steric effects of the phosphine ligands are completely negligible due to the small size of PH_3 .³² In the isolated catalyst, the five-membered ring formed by the ethylenediamine ligand and the Ru center adopts a puckered geometry, with equivalent λ and δ configurations, which can readily interconvert. In our previous computational study,¹⁶ hydrogenation was assumed to occur involving only one of the two different types of NH proton. We here revisit the potential energy surface for acetone hydrogenation taking both the axial (ax) and equatorial (eq) types of approach into account (see Figure 1 and Table 1). For acetophenone, there are in fact *four* modes of approach. Proton transfer can occur from the axial or equatorial NH group. Also, for each of those cases, the more bulky phenyl group can be oriented away from or toward the closer phosphine ligand. We refer in Figure 1 to this second pair of orientations as "out" and "in", respectively, as, for example, in the ax-out TS.

For the case of acetone and axial approach, the computed potential energy surface for the catalytic cycle of Scheme 1, shown in Figure 2, is very similar to the surface presented previously.¹⁶ Starting from the roughly octahedral catalyst

(26) Jaguar 5.0; Schrödinger, L. L. C.: Portland, OR, 1991–2003.

(27) Frisch, M. J.; Trucks, G. W.; Schlegel, H. B.; Scuseria, G. E.; Robb, M. A.; Cheeseman, J. R.; Montgomery, J. A., Jr.; Vreven, T.; Kudin, K. N.; Burant, J. C.; Millam, J. M.; Iyengar, S. S.; Tomasi, J.; Barone, V.; Mennucci, B.; Cossi, M.; Scalmani, G.; Rega, N.; Petersson, G. A.; Nakatsuji, H.; Hada, M.; Ehara, M.; Toyota, K.; Fukuda, R.; Hasegawa, J.; Ishida, M.; Nakajima, T.; Honda, Y.; Kitao, O.; Nakai, H.; Klene, M.; Li, X.; Knox, J. E.; Hratchian, H. P.; Cross, J. B.; Bakken, V.; Adamo, C.; Jaramillo, J.; Gomperts, R.; Stratmann, R. E.; Yazyev, O.; Austin, A. J.; Cammi, R.; Pomelli, C.; Ochterski, J. W.; Ayala, P. Y.; Morokuma, K.; Voth, G. A.; Salvador, P.; Dannenberg, J. J.; Zakrzewski, V. G.; Dapprich, S.; Daniels, A. D.; Strain, M. C.; Farkas, O.; Malick, D. K.; Rabuck, A. D.; Raghavachari, K.; Foresman, J. B.; Ortiz, J. V.; Cui, Q.; Baboul, A. G.; Clifford, S.; Cioslowski, J.; Stefanov, B. B.; Liu, G.; Liashenko, A.; Piskorz, P.; Komaromi, I.; Martin, R. L.; Fox, D. J.; Keith, T.; Al-Laham, M. A.; Peng, C. Y.; Nanayakkara, A.; Challacombe, M.; Gill, P. M. W.; Johnson, B.; Chen, W.; Wong, M. W.; Gonzalez, C.; Pople, J. A. *Gaussian 03*, Revision C.02; Gaussian, Inc.: Wallingford, CT, 2004.

(28) Hay, P. J.; Wadt, W. R. *J. Chem. Phys.* **1985**, *82*, 720.

(29) (a) Foster, J. P.; Weinhold, F. *J. Am. Chem. Soc.* **1980**, *102*, 7211.

(b) Reed, A. E.; Weinhold, F. *J. Chem. Phys.* **1983**, *78*, 4066. (c) Reed, A. E.; Weinstock, R. B.; Weinhold, F. *J. Chem. Phys.* **1985**, *83*, 735. (d) Reed, A. E.; Weinhold, F. *J. Chem. Phys.* **1985**, *83*, 1736.

(30) Grimme, S. *J. Chem. Phys.* **2003**, *118*, 9095–9102.

(31) Grimme, S. *J. Phys. Chem. A* **2005**, *109*, 3067–3077.

(32) Tolman, C. A. *Chem. Rev.* **1977**, *77*, 313–348.

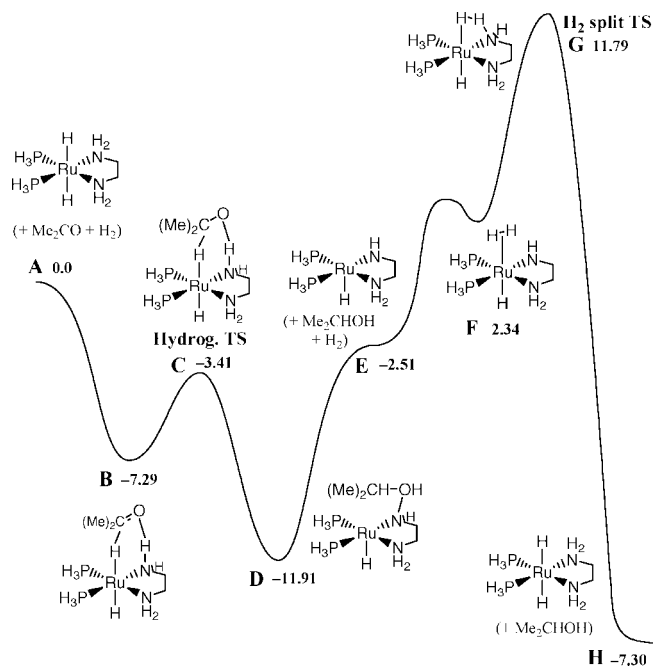


Figure 2. Calculated B3LYP/6-31G* potential energy surface (energies in kcal/mol) for the catalytic cycle of hydrogenation of acetone by the $\text{RuH}_2(\text{PH}_3)_2(\text{en})$ model catalyst (with transfer of the axial NH proton).

species (**A**), a weak complex (**B**) is formed with the ketone, with hydrogen bonding to oxygen from the axial NH group ($r_{\text{OH}} = 2.03 \text{ \AA}$) and a very weak interaction between the ruthenium hydride and the carbonyl C atom ($r_{\text{HC}} = 2.92 \text{ \AA}$). In solution, interactions between solvent and the separated reactants will lessen the importance of this weak complex. Indeed, calculations using a continuum model of benzene solvent show that species **B** lies only 1.6 kcal/mol lower in energy than reactants, as compared to 7.1 kcal/mol in the gas phase. Entropic effects also mean that the complex will be higher in free energy terms than reactants.

The hydrogenation TS (**C**) involves concerted transfer of the hydride (r_{RuH} , which is 1.72 \AA in **A** and **B** and increases to 1.76 \AA in **C**, while r_{HC} decreases from 2.92 \AA in **B** to 1.81 in **C**) and the proton (r_{NH} is 1.02 \AA in **A** and **B** and increases to 1.03 \AA in **C**, while r_{OH} decreases from 2.03 \AA in **B** to 1.82 \AA in **C**). A product complex is then formed, with hydrogen bonding of the formed alcohol to the basic amido nitrogen atom ($r_{\text{NH}} = 1.77 \text{ \AA}$). Loss of alcohol leads to the amido complex (**E**), which, as discussed in our previous work,¹⁶ has a near-planar amido nitrogen center, indicating $\text{Ru}=\text{N}$ double-bond character. Addition of H_2 then forms a weakly bound dihydrogen complex (**F**), with heterolytic splitting of dihydrogen through transition state **G** ($r_{\text{RuH}} = 1.88 \text{ \AA}$ vs 1.95 \AA in **F**, $r_{\text{HH}} = 0.99 \text{ \AA}$ vs 0.78 \AA in **F**, $r_{\text{NH}} = 1.40 \text{ \AA}$ vs 2.46 \AA in **F**), leading back to the starting dihydride catalyst. The splitting of dihydrogen represents the turnover-limiting step.

Table 1 presents the calculated relative energies for the different species in the catalytic cycle for the two isomeric pathways involved in hydrogenation of acetone and the four isomeric pathways for acetophenone. There is growing evidence that in some cases B3LYP can lead to poor computed energies,

especially for systems containing transition metals,³³ but also for simple organic systems.³⁴ In our previous study,¹⁶ we checked that energetics in the present system are not very sensitive to the basis set used or the functional (B3LYP vs BP86). We have carried out new tests here, which again suggest that the effect of changing basis set and method is modest. Indeed, the Hartree–Fock and standard MP2 energies (not shown in Table 1) are fairly similar to the spin-component-scaled^{30,31} MP2 (SCS-MP2) results, showing that correlation effects are not too large in this system. Unlike for first-row transition metal compounds, such small correlation effects are relatively common for compounds containing second- or third-row transition metals. The most noticeable difference between the B3LYP and SCS-MP2 results is that the two transition states lie roughly 3 kcal/mol higher in energy with the SCS-MP2 method compared to B3LYP.

Relative to separated reactants, the TS for hydrogenation of acetone involving the H_{ax} proton lies 1.91 kcal/mol lower in energy than the one involving the H_{eq} proton. Reaction involving transfer of the axial proton appears to be favored for geometric reasons, as expected on the basis of the nature of the TS. Concerted transfer of a hydride and a proton is expected to proceed most favorably in a TS with a near-planar arrangement of the accepting $\text{C}=\text{O}$ bond and the donor $\text{H}-\text{Ru}-\text{N}-\text{H}$ moiety. In the dihydride catalyst, the $\text{H}-\text{Ru}-\text{N}-\text{H}_{\text{ax}}$ dihedral angle is 17.0°, and the corresponding angle at the hydrogenation TS is 6.9°, with an $\text{H}-\text{C}-\text{O}-\text{H}_{\text{ax}}$ dihedral angle of 26.0°, all corresponding to the ideal near-planar arrangements. A much larger angle of 48.5° is found for the $\text{H}-\text{Ru}-\text{N}-\text{H}_{\text{eq}}$ dihedral in the isolated catalyst, and the corresponding TS is much less close to planar than the one involving the axial proton, with $\text{H}-\text{Ru}-\text{N}-\text{H}_{\text{eq}}$ and $\text{H}-\text{C}-\text{O}-\text{H}_{\text{eq}}$ dihedral angles of 26.1° and 13.7°, respectively.

Considering the four possible hydrogenation TSs with the prochiral acetophenone substrate, it can be seen first of all that the preference for transfer of the axial NH proton is maintained. The two lowest TSs, lying respectively 3.20 and 2.77 kcal/mol lower in energy than reactants, involve the axial protons, with the other TSs lying 1 to 2 kcal/mol higher in energy. As expected, the small steric bulk of the PH_3 ligands means that the TSs with *in* and *out* approach are very similar in energy, especially where H_{ax} is being transferred. There does however appear to be a slight preference for the *out* mode of approach, as it lies lower in energy for both the H_{ax} and H_{eq} cases. Steric repulsion between the more bulky phenyl group and the phosphines in the TSs with the *in* mode of approach may explain this preference. A more convincing explanation is that a weak electrostatic interaction between the aryl ring of the ketone and a proton on the NH_2 group not involved directly in the reaction stabilizes the *out* TSs. This interaction has been suggested to

(33) (a) See for example: Reiher, M.; Salomon, O.; Hess, B. A. *Theor. Chem. Acc.* **2001**, *107*, 48–55. (b) Carreón-Macedo, J.-L.; Harvey, J. N. *J. Am. Chem. Soc.* **2004**, *126*, 5789–5797. (c) Schultz, N. E.; Zhao, Y.; Truhlar, D. G. *J. Phys. Chem. A* **2005**, *109*, 4388–4403. (d) Schultz, N. E.; Zhao, Y.; Truhlar, D. G. *J. Phys. Chem. A* **2005**, *109*, 11127–11143. (e) Furche, F.; Perdew, J. P. *J. Chem. Phys.* **2006**, *124*, 044103. (f) Harvey, J. N. *Ann. Rep. Prog. Chem., Sect. C* **2006**, *102*, 203–226.

(34) (a) See for example: Alder, R. W.; Blake, M. E.; Chaker, L.; Harvey, J. N.; Paolini, F.; Schütz, J. *Angew. Chem., Int. Ed.* **2004**, *43*, 5896–5911. (b) Grimme, S. *Angew. Chem. Int. Ed.* **2006**, *45*, 4460–4464. (c) Wodrich, M. D.; Corminboeuf, C.; Schleyer, P. v. R. *Org. Lett.* **2006**, *8*, 3631–3634. (d) Schreiner, P. R.; Fokin, A. A.; Pascal, R. A.; de Meijere, A. *Org. Lett.* **2006**, *8*, 3635–3638. (e) Friesner, R. A.; Knoll, E. H.; Cao, Y. *J. Chem. Phys.* **2006**, *125*, 124107. (f) Grimme, S.; Steinmetz, M.; Korth, M. *J. Org. Chem.* **2007**, *72*, 2118–2126.

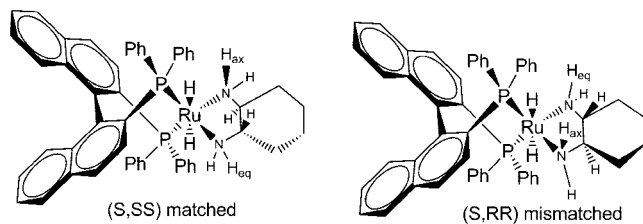


Figure 3. Structure of the matched $\text{RuH}_2(\text{S-BINAP})(\text{S,S-cydn})$ and mismatched $\text{RuH}_2(\text{S-BINAP})(\text{R,R-cydn})$ catalysts.

play a role in defining selectivity.^{20,35} The shortest H—C contact of this type is 3.25 Å in the ax-out TS and 2.88 Å in the eq-out TS. The latter value in particular indicates significant interaction and may explain why the eq-out TS is only 1.10 kcal/mol less stable at the B3LYP/6-31G* level than the ax-out TS, whereas the difference in energy between the eq and ax TSs in the acetone reactions is 1.91 kcal/mol. For the *in* TSs, the corresponding distance is very large.

As noted above, the predicted rate-limiting step based on Figure 2 and Table 1 is H_2 addition through TS **G**. This agrees with experimental observations for the $\text{RuH}_2(\text{BINAP})(\text{tmen})$ and $\text{RuH}_2(\text{PPh}_3)_2(\text{tmen})$ systems.¹⁶ However, the quite large energy barrier of ca. 15 kcal/mol calculated here and previously¹⁶ is inconsistent with the measured¹⁶ activation enthalpy of ca. 8 kcal/mol in benzene. It is also inconsistent with the high enantioselectivity of hydrogenation with these catalysts, as the calculations suggest that racemization of the product by reversing the steps from **A** to **E** would be faster than hydrogen addition through **G**. Although the three computational methods used here give similar barriers, it is possible that some errors in the calculations exaggerate the energy of barrier **G** relative to that of the hydrogenation barrier **C**. It is also possible that in the more polar solvents often used for enantioselective catalysis, another, lower energy, mechanism for converting **E** to **A** exists in which **F** is protonated on the amido nitrogen by solvent, then the dihydrogen ligand is deprotonated. Some evidence for this is available from experiment, as the protonated form of **F** can be detected in solution.^{20,36}

B. Reaction of Acetophenone with the Experimental Matched $\text{Ru}(\text{S-Binap})(\text{S,S-cydn})$ System. We now turn to our results for the much larger realistic system. We consider first the “matched”³⁷ $\text{Ru}(\text{S-Binap})(\text{S,S-cydn})$ catalyst shown on the left in Figure 3. This leads to formation of *R* alcohol with ketones such as acetophenone, with good enantioselectivity. Note that we have located only a small number of the complexes **B**, **D**, and **F** for the real system and do not include the results here. As discussed above, these weakly bound species are unimportant in solution. The key geometrical parameters for the different stationary points are rather similar to those described above for the model system. For example, the Ru—H distance is 1.72 Å in the catalyst species **A** (identical to the value in the model system) and increases to 1.83 Å in the ax-out hydrogenation TS **C** (1.76 Å for the model system). The other geometrical properties of this hydrogenation TS are also very similar to those noted above for the model system: r_{HC} for the transferring hydride is 1.81 Å (1.81 Å in the model), r_{NH}

and r_{HO} for the transferring proton are 1.03 and 1.88 Å (1.03 and 1.82 Å for the model), and the HRuNH dihedral is 3.3° (6.9° for the model system).

The energies of the different species in the catalytic cycle (see Table 2) are also by and large similar to those obtained for the model system. The turnover-limiting step is still predicted to be heterolytic splitting of dihydrogen, with the corresponding TS **G** lying 13.32 kcal/mol above the amido complex **E**, very similar to the 14.30 kcal/mol separating these species in the model system. As noted above, the effective barrier for H_2 splitting needs to be lower than this for enantioselective catalysis to occur, so that hydrogenation of **E** dominates over the competing racemization of alcohol occurring through reversion to **A**. It is possible that the computations exaggerate the barrier height for **G**, but it is also possible that an alternative pathway accounts for the efficient H_2 splitting and involves proton transfer with solvent.^{20,36}

Unlike for the model systems, B3LYP/6-31G* calculations predict the ketone hydrogenation step to have a positive activation energy, with TS **C** lying 3.89 kcal/mol above the separated catalyst and ketone reagents in the case of the ax-out approach. This contrasts with relative energies of -3.41 and -3.20 kcal/mol for the corresponding hydrogenation TSs of acetone and acetophenone with the model system. The slightly increased barrier could be readily explained by the increased steric bulk of the real system.

It is to be noted that in this case the SCS-MP2 method predicts a lower barrier, more similar to that obtained with the model system. It is difficult to decide which method gives the more accurate barrier for such a large system (120 atoms, 572 explicitly described electrons, 825 basis functions with the 6-31G* basis, 1536 basis functions with the 6-311G** basis), as both methods could in principle lead to errors. For example, the B3LYP method does not describe nonbonding dispersion interactions well.³⁸ Such interactions may stabilize the TS relative to reactants, due to nonbonding contacts between the methyl and phenyl groups of the substrate and the BINAP and cydn ligands. Equally, the SCS-MP2 method, which can describe such interactions, will not do so very accurately with the 6-31G* basis due to significant basis set superposition error that may artificially stabilize the TS. Also, as mentioned before, solvent effects would need to be taken into account to obtain results that could be compared with experiment in quantitative terms.

In any case, both methods predict a small barrier to hydrogenation of ketones, in agreement with the known high reactivity of these catalysts. Furthermore, as discussed below, both methods, as well as the B3LYP calculations with the 6-311G** basis, predict the same order for the relative energies of the four isomeric TSs, with fairly similar energy gaps between them. Since these energy gaps are the key factors for determining selectivity, the slight uncertainty associated with calculating the exact absolute barrier heights for these reactions is not a major problem. Overall, the good similarity between the qualitative features of the reaction emerging from the study of the model system and the real system provides retrospective validation for the use of the model in the earlier work.³⁸ The nature and chirality of the diphosphine and diamine ligands does not seem to affect the fundamental bonding pattern in the intermediates and TSs in a significant way.

We now consider the different transition states and the expected enantioselectivity. Considering the C_2 symmetry of the catalyst, the two enantiotopic faces of the ketone, and the

(35) A related H-bond has been suggested to play a role in enantioselective hydrogenation of acetylthiophene. See: Cao, P.; Zhang, X. M. *J. Org. Chem.* **1999**, *64*, 2127–2129.

(36) Evidence for a related mechanism is also provided in: Sandoval, C. A.; Ohkuma, T.; Utsune, N.; Tsutsumi, K.; Murata, K.; Noyori, R. *Chem. As. J.* **2006**, *102*.

(37) Masamune, S.; Choy, W.; Petersen, J. S.; Sita, L. R. *Angew. Chem., Int. Ed. Engl.* **1985**, *24*, 1–30.

(38) See for example: Grimme, S. *J. Comput. Chem.* **2004**, *25*, 1463–1473.

Table 2. B3LYP/6-31G* Energies (kcal/mol) Relative to Reactants for the Species in the Catalytic Cycles for Hydrogenation of Acetophenone by the RuH₂(S-BINAP)(S,S-cydn) Real Catalyst (species labels refer to Figure 2)^a

	acetophenone			
	ax-out	ax-in	eq-out	eq-in
A	0.00	0.00	0.00	0.00
C	3.89 (-6.05) (6.29)	5.77 (-2.40) (7.95)	7.90 (1.25) (10.32)	9.39 (2.50) (11.38)
E	4.29 (1.92)	4.29 (1.92)	2.94 (0.46)	2.94 (0.46)
G	17.61	17.61	18.38	18.38
H	-5.46 (-7.51) (-5.76)	-5.46 (-7.51) (-5.76)	-5.46 (-7.51) (-5.76)	-5.46 (-7.51) (-5.76)

^a SCS-MP2/6-31G* (in bold) and B3LYP/6-311G** (in italics) relative energies are shown for selected species.

availability of axial and equatorial protons, we need to consider four TSs, as for the model system. Two TSs lead to *R* alcohol and two to *S* alcohol. The BINAP ligand is fairly rigid, and the cyclohexane ring locks the cydn ligand into a single conformer, so it is unlikely that other low-energy conformers of the catalyst exist that could lead to alternative TSs. Indeed, only fairly small changes in orientation of the P-phenyl groups on the BINAP ligand are noted for the transition states. The *cis*-dihydride isomer identified in other related systems could be in equilibrium with the *trans*-dihydride, but it is a less active catalyst so would not be expected to contribute significantly to the enantioselectivity.²³

As shown in Table 2, the ax-out TS is preferred at all levels of theory. This TS is expected to lead to phenethyl alcohol with *R* chirality, and this is indeed the experimentally observed major product. Of the other TSs, the ax-in and eq-out TSs would be expected to yield the other enantiomer of the product, and the lower of the two, the ax-in TS, lies 1.87 kcal/mol higher in energy than the ax-out TS at the B3LYP/6-31G* level. The ax-in TS is second lowest in energy at the B3LYP/6-311G**//LYP/6-31G*, and SCS-MP2/6-31G**//B3LYP/6-31G* levels of theory also, lying respectively 1.67 and 3.65 kcal/mol above the ax-out TS. The B3LYP values are consistent with the observed enantiomeric excess of 97% at 298 K in reactions of the similar catalyst RuCl₂{(S)-BINAP}{(S,S)-dpn} with the similar substrate 1'-acetonephthone,¹ or the 80% ee obtained for hydrogenation of acetophenone.⁶ A difference in the free energy of activation of 1.87 kcal/mol at 298 K would lead to an enantioselectivity of 92%. The calculated difference in the energies of activation should be similar to the difference in the free energies of activation.³⁹ Although the absolute accuracy of the B3LYP and SCS-MP2 methods is much lower than that needed to predict the energy difference between the two TSs in a reliable way, the good result here is not unexpected given that the errors in the two calculations are likely to be similar and thereby cancel out.⁴⁰

Inspection of the structures of the different TSs suggests that the observed energy ordering can largely be explained on the basis of the steric model of Chart 1 together with the preference, already noted for the small model system, for transfer of the axial NH₂ proton. The steric interactions can be shown more

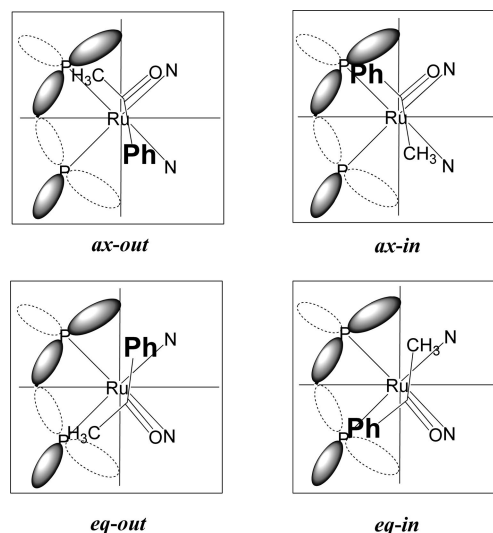


Figure 4. Quadrant diagrams for the hydrogenation TS of acetophenone by the matched (S-BINAP)RuH₂(S,S-cydn) catalyst. The substrate is above the P₂RuN₂ plane of the catalyst. The gray oval lobes represent BINAP phenyl or naphthyl rings situated above the plane, with the dashed lobes representing lobes situated below the plane. This diagram also applies for the S,RR catalyst, provided the ax and eq labels are switched.

clearly using a quadrant diagram (Figure 4) of the four competing TSs. As shown, and noted previously, the C=O bond is almost in the same plane as the Ru–N bond and the two transferring H moieties in the TS. As a result, the two substituents on the ketone are oriented respectively *in* toward the upper-left or lower-left quadrant of the BINAP ligand, or *out* toward the bottom or top of the system, further away from the BINAP ligand. In the case of the matched RuH₂{(S)-BINAP}{(S,S)-cydn} catalyst, the relative stereochemistry of the diamine and the BINAP is such that the axial proton is in the upper-right quadrant and the equatorial proton is in the lower-right quadrant. Also, a pseudo-equatorial phenyl group and the naphthyl group from the BINAP are situated in the upper-left quadrant, with a pseudoaxial phenyl group from the other phosphorus atom occupying the lower-left quadrant. The ax-out approach minimizes steric interactions. The smaller methyl group does not approach the phenyl (shortest C–C distance, 3.79 Å) or naphthyl groups of the BINAP (shortest C–C contact, 4.39 Å) too closely, and the phenyl substituent is oriented mostly away from the pseudoaxial phenyl group of the BINAP (shortest C–C distance, 3.72 Å).

The ax-in approach is much less favorable, as it brings the more bulky phenyl substituent close to the pseudo-equatorial phenyl group (shortest C–C contact, 3.57 Å) and the naphthyl backbone (shortest C–C contact, 3.84 Å). This explains the higher energy for this TS. The two TSs involving the equatorial proton, eq-out and eq-in, are intrinsically higher in energy, as this proton gives a less favorable TS geometry (the HRuNH

(39) It is possible to compute the difference in the free energies of activation for the two TSs at the B3LYP/6-31G* level, using expressions for the partition functions based on the rigid rotor/harmonic oscillator approximation, and this yields a difference of 2.03 kcal/mol. This value is not necessarily a closer approximation to the true difference in free energies of activation than is the difference in the energies of activation, given the errors involved in applying gas-phase rigid rotor/harmonic oscillator expressions to the reaction in solution, but it is satisfying to note $\Delta\Delta G^\ddagger$ is similar to $\Delta\Delta E^\ddagger$.

(40) (a) For previous examples of this error cancellation in prediction of selectivity for complex systems, see: Harvey, J. N.; Aggarwal, V. K.; Bathelt, C. M.; Carreón-Macedo, J.-L.; Gallagher, T.; Holzmann, N.; Mulholland, A. J.; Robiette, R. J. *Phys. Org. Chem.* **2006**, *19*, 60. (b) Robiette, R.; Richardson, J.; Aggarwal, V. K.; Harvey, J. N. *J. Am. Chem. Soc.* **2006**, *128*, 2394.

Table 3. B3LYP/6-31G* Energies (kcal/mol) Relative to Reactants for the Species in the Catalytic Cycles for Hydrogenation of Acetophenone by the RuH₂(*S*-BINAP)(*R,R*-cydn) Mismatched Catalyst (species labels refer to Figure 2)^a

	acetophenone			
	ax-out	ax-in	eq-out	eq-in
A	0.00	0.00	0.00	0.00
C	6.29 (-2.15) (9.45)	8.15 (1.52) (10.92)	5.65 (-4.14) (8.32)	9.72 (1.26) (12.37)
E	1.70	1.70	6.37	6.37
G	16.29	16.29	20.64	20.64
H	-5.46 (-7.51) (-5.76)	-5.46 (-7.51) (-5.76)	-5.46 (-7.51) (-5.76)	-5.46 (-7.51) (-5.76)

^a SCS-MP2/6-31G* (in bold) and B3LYP/6-311G** (in italics) relative energies are shown for selected species.

dihedral angle in these two TSs are respectively 24.7° and 22.2°, much further from the ideal near-zero value found in the model system than are the values of 3.3° and 0.6° for the ax-out and ax-in TSs). Additionally, these two TSs include significant unfavorable steric interactions between the ketone substituent located in the lower-left quadrant and the pseudoaxial phenyl group of the BINAP (the shortest C–C contact is respectively 3.42 and 3.58 Å).

As discussed for the model system, the TSs in which the phenyl group is oriented *out* can also be stabilized by hydrogen bonding between the phenyl ring and the NH₂ proton of the amino group of the diamine not involved in hydrogen transfer. In fact, this interaction seems to be larger in the present case, perhaps because the far greater steric repulsion of the BINAP ligand compared to the PH₃ ligands in the model system pushes the acetophenone moiety closer to the diamine. Hence the shortest C–H contact is 2.65 Å in the ax-out TS (versus 3.25 Å in the model system) and 2.99 Å in the eq-out TS (versus 2.88 Å in the model system). This interaction may play a role in favoring the ax-out TS over the ax-in TS, in which the interaction is absent.^{20,35} Nonclassical hydrogen bonding between a hydrogen bond donor and an aromatic ring is well-known. For example, ammonium ions bind by almost 20 kcal/mol to benzene in the gas phase,⁴¹ and this interaction is predicted to persist even in water.⁴² The interaction between ammonia and benzene is weaker, on the order of 2 kcal/mol.⁴³ The interaction in the present system is likely to be fairly weak also, because although coordination to ruthenium polarizes the N–H bond, and hence strengthens the interaction, the geometry is also not ideal. A rough estimate of the contribution of this interaction can be obtained from the differences in the energies of the ax-out and ax-in, and eq-out and eq-in, TSs in the model system (Table 1, 0.43 and 1.09 kcal/mol, respectively).

It is interesting to note in this context that hydrogenation of dialkyl ketones, for which this hydrogen bonding cannot occur, tends to give much lower enantioselectivities.⁸ Very bulky BINAP derivatives (e.g., XylBINAP, which has 3,5-dimethylphenyl groups on phosphorus instead of phenyl groups) are needed to obtain reasonable ee's, even when the steric bulk of the two ketones groups is very different.

C. Reaction of Acetophenone with the Experimental Mismatched Ru(*S*-Binap)(*R,R*-cydn) System. Additional insight into the origin of selectivity and catalyst design can be obtained by considering the corresponding results obtained for the mismatched RuH₂(*S*-BINAP)(*R,R*-cydn) system (see Figure 3 above) reacting with acetophenone. In reactions with acetophenone, this is known² to give preferentially the same *R* enantiomer of the corresponding 1-naphthyl ethanol as obtained

with the matched *S,SS* catalyst, but with a drastically reduced ee of 14% instead of 97%. The geometry of the BINAP ligand in the *S,RR* catalyst is almost the same as in the matched *S,SS* catalyst. The chirality of the two nitrogen-bearing carbons in the cyclohexanediamine ligand is however changed. As the cydn ligand is locked into a conformation in which the two amino groups are equatorial, this is equivalent to changing the conformation of the five-membered (RuNCCN) ring from λ to δ , or equivalently, to switching the position of the axial and equatorial protons in the quadrant diagram of Figure 4, without changing the position of the BINAP ligand. We have optimized the geometry of the four TSs involved in hydrogenation of acetophenone at the B3LYP/6-31G* level and present the energies in Table 3.

As can be seen, the transition states lie at roughly similar energies relative to reactants as in the matched case, and the geometries of the TSs are similar also. However, the relative ordering of the isomeric TSs is different, with the eq-out TS now lying lowest in energy with all methods. The next lowest TS is the ax-out TS, lying 0.64 kcal/mol (B3LYP/6-31G*) higher in energy. This is in fair agreement with the experimental observation concerning the magnitude and the sign of the enantiomeric excess. The eq-out TS leads to *R* alcohol, whereas the ax-out TS leads to *S* alcohol. Hence the 0.64 kcal/mol difference in energy between the two TSs, with the eq-out TS lying lower in energy, would give an ee for the *R* alcohol of 49%, compared to 13% observed experimentally.¹ For such low ee's, small errors in the calculations can lead to large errors on the ee, as shown by the fact that a difference in free energy of activation of 0.15 kcal/mol, only 0.5 kcal/mol different from the calculated difference between the energies of activation, is needed to account for an ee of 13%. The calculations reported here are certainly not accurate to within such small amounts. The SCS-MP2 and B3LYP/6-311G** levels of theory also predict the second-lowest TS to be the ax-out isomer, with slightly larger energy gaps of 1.99 and 1.13 kcal/mol. While these energy differences would predict a larger ee than is observed experimentally, it is noteworthy that the energy gap with these two methods is smaller than it was for the matched system (respectively 3.65 and 1.67 kcal/mol), consistent with the lower enantioselectivity obtained with the mismatched catalyst.

The relative energy of the different TSs can be understood with reference to the same quadrant diagram (Figure 4) as before. However, for the *S,RR* catalyst, the TS geometries involving the equatorial NH protons correspond to those labeled "ax" in Figure 4, and vice versa. The lowest-energy eq-out TS thereby corresponds to the sterically most favorable TS, with relatively large distances between the phenyl and methyl substituents of the acetophenone substrate and the phenyl and naphthyl groups of the BINAP ligand. The shortest C–C contact is 3.80 Å, between the ketone methyl group and the pseudoaxial phenyl of the BINAP ligand in the lower-left quadrant. This

(41) Deakynne, C. A.; Meot-Ner, M. *J. Am. Chem. Soc.* **1985**, *107*, 474–479.

(42) Sa, R.; Zhu, W.; Shen, J.; Gong, Z.; Cheng, J.; Chen, K.; Jiang, H. *J. Phys. Chem. B* **2006**, *110*, 5094–5098.

(43) See for example: Vaupel, S.; Brutschy, B.; Tarakeshwar, P.; Kim, K. S. *J. Am. Chem. Soc.* **2006**, *128*, 5416–5426.

distance does not appear to be short in Figure 4, but the ketone in this case is rotated somewhat anticlockwise to minimize steric interactions. However, this TS involves the unfavorable equatorial proton, with a HRuNH dihedral angle of 25°, far from the preferred planar geometry. In contrast, the ax-out TS involves a favorable orientation of the transferring hydride–proton array (HRuNH dihedral angle of 0°). As found for the TSs involving the equatorial proton for the matched catalyst, however, this TS is unfavorable for steric reasons, due to interaction between the ketone methyl group and the pseudoaxial phenyl group of the BINAP ligand, with a shortest contact of 3.44 Å. The TSs in which the phenyl group on the ketone is oriented *in*, toward the BINAP ligand, lie higher in energy. In the ax-in TS, there are several close contacts (3.65 Å) between the ketone phenyl substituent and the pseudoaxial phenyl group in the lower-left quadrant of Figure 4. In the eq-in TS, the most unfavorable contact is between the ketone phenyl and the BINAP pseudo-equatorial phenyl, with a C–C distance of 3.54 Å. This TS is of course also destabilized by the involvement of the less reactive equatorial proton.

As for the matched system, as well as the steric and electronic effects already mentioned, hydrogen bonding between the adjacent NH₂ group and the phenyl ring of the acetophenone reactant could also play a role in stabilizing the two *out* TSs. The pseudoequatorial phenyl group on the BINAP ligand prevents close approach of the phenyl group to the cydn ligand in the ax-out TS, and the shortest H–C contact is as long as 3.86 Å. However, for the eq-out TS, a very short contact of 2.59 Å is present, indicating substantial electrostatic stabilization of this TS, on top of the favorable steric environment. This presumably explains why this is the lowest energy TS for the mismatched system, despite the intrinsically unfavorable involvement of the equatorial NH₂ proton.

It is interesting to note from Table 3 that if the only reaction pathways available for hydrogenation involved the axial NH proton, the lowest TS would be the ax-out TS (which leads to *S* alcohol), with a gap relative to the next lowest TS, the ax-in TS (which leads to *R* alcohol), of 1.87 kcal/mol (B3LYP/6-31G*, 1.48 kcal/mol with 6-311G**), somewhat more than the gap that in fact occurs between the two lowest TSs, eq-out and ax-out, of 0.63 kcal/mol (1.12 kcal/mol with 6-311G**). This would then lead to a predicted enantioselectivity different in sign and, at least with the 6-31G* basis, also in magnitude from what is observed experimentally. Even with the expected inaccuracies in the calculations, this conclusion should be robust and demonstrates the potential importance of hydrogenation involving the equatorial NH protons in this type of catalysis.

D. Comparison of Matched and Mismatched (BINAP)-RuH₂(cydn) Catalysts. To summarize the results from the matched and mismatched systems, we have calculated the barrier height for the four modes of approach of acetophenone to both the matched and mismatched catalysts. The calculated barrier heights are consistent with the observed enantioselectivities. We have discussed the energies of the TSs based on three factors. First, there is an intrinsic electronic factor whereby involvement of the H_{ax} proton on nitrogen is preferable to involvement of the H_{eq} proton. Next, steric interaction between the phenyl group of the ketone and the phenyl and naphthyl groups on the BINAP ligand tends to disfavor most of the TSs, except the ax-out TS for the matched system and the eq-out TS for the mismatched system. Finally, hydrogen bonding between the second NH₂ group of the diamine and the phenyl group of the ketone can act to stabilize most of the *out* TS structures. Taken together, these effects rationalize the TS energies and help to explain the

Table 4. Relative Energies (in kcal/mol at the B3LYP/6-311G level of theory) of the Different TSs for Hydrogenation of Acetophenone by RuH₂(S-BINAP)(S,S-cydn) and RuH₂(S-BINAP)(R,R-cydn), Favorable (+) and Unfavorable (–) Electronic and Steric Effects on TS Energy, and Expected Chirality from Each TS**

<i>S,SS</i>	<i>E</i> _{rel}	electronic	steric	H-bond	chirality
ax-out	0.00	+	+	+	<i>R</i>
ax-in	1.67	+	–	/	<i>S</i>
eq-out	4.04	–	–	+	<i>S</i>
eq-in	5.10	–	–	/	<i>R</i>
<i>S,RR</i>	<i>E</i> _{rel}	electronic	steric	H-bond	chirality
ax-out	1.13	+	–	/	<i>S</i>
ax-in	2.60	+	–	/	<i>R</i>
eq-out	0.00	–	+	+	<i>R</i>
eq-in	4.05	–	–	/	<i>S</i>

selectivity.⁴⁴ The relative energies of the four key TSs are shown in Table 4. This table also shows how the energy of each TS is affected by steric effects, by the electronic factor linked with transfer of the equatorial or axial NH protons, and by the hydrogen bonding. Finally, the table includes the chirality of the alcohol that would be produced by each TS.

Further instructive conclusions can be derived from noting that the *S,SS* and *S,RR* catalysts are of course isomers. It is therefore possible to combine the data in Tables 2 and 3 and to compare the energies of the catalysts and of the TSs. For the (BINAP)Ru(H)₂(cydn) system, this comparison is not meaningful, as there is no available low-energy pathway to convert any of the species involved in the catalytic cycle for the *S,SS* catalyst into the corresponding *S,RR* species (or, equivalently, the *R,SS* or *R,RR* species). However, analogous interconversions are possible for related systems that have been used in catalysis. First, it has been observed that (BINAP)Ru(H)₂(en) and (Ph₃P)₂Ru(H)₂(dppe) lead to hydrogenation of acetophenone with moderate enantioselectivities, of 57 and 73%, respectively.¹ The ethylenediamine ligand (en) is not conformationally rigid, so that for the (BINAP)Ru(H)₂(en) catalyst ready interconversion of the λ and δ conformations of the RuNCCN five-membered ring can occur, leading to geometries analogous to the *S,SS* and *S,RR* forms discussed here. For (Ph₃P)₂Ru(H)₂(dppe) the dominant contribution to catalysis is from the isomer in which the two hydride ligands lie *trans* to each other,²³ which has a similar geometry to the BINAP systems considered here. In particular, the two triphenylphosphine ligands in this isomer can be expected to adopt conformations similar to those observed for the BINAP ligand. Two conformations, respec-

(44) In a recent computational study of enantioselectivity in hydrogenation of acetophenone by (SxylBINAP)RuH₂(S,S-dpen),⁴⁵ a different explanation has been given for the selectivity. The hydrogen transfer TSs located in this study are similar to those obtained here. The authors have also located weak hydrogen-bonded complexes between the dihydride catalyst and the ketone, similar in geometry to the intermediate **B** shown in Figure 2. As discussed above, such minima are likely to disappear in the presence of solvent and when taking entropic factors into account, so should not play an important role in the mechanism. However, in the case of the ax-out approach only, the authors located a second stable intermediate in which the ketone has moved closer to the transferring hydride and suggest that the presence of this stable species helps to explain the selectivity. No such minimum has been found in the present case, perhaps because the less bulky BINAP ligand was modeled instead of XylBINAP. Since BINAP gives a similar pattern of stereoselectivity to XylBINAP, it is unlikely that any major effect is present with the latter ligand that is absent with BINAP. The appearance of the energy plot in ref 41 (Figure 2) suggests a conformational change, perhaps in the bulky xyl sidechains, upon approach of the ketone. Such a change is unlikely to be rate-determining since it can also occur before the ketone binds.

(45) French, S. A.; Di Tommaso, D.; Zanotti-Gerosa, A.; Hancock, F.; Catlow, C. R. A. *Chem. Commun.* **2007**, 2381–2383.

Table 5. Relative Energies (kcal/mol) for the Different TSs for Hydrogenation of Acetophenone by RuH₂(BINAP)(cydn) Isomers, at the B3LYP/6-31G*, SCS-MP2/6-31G*, and B3LYP/6-311G Levels of Theory^a**

	B3LYP/6-31G*	SCS-MP2/6-31G*	B3LYP/6-311G**
catalyst	0.00 (-0.40)	0.00 (-0.11)	0.00 (1.28)
ax-out TS	3.89 (5.88)	-6.05 (-2.25)	6.29 (10.73)
ax-in TS	5.77 (7.75)	-2.40 (1.41)	7.95 (12.20)
eq-out TS	7.90 (5.25)	1.25 (-4.25)	10.32 (9.60)
eq-in TS	9.39 (9.32)	2.50 (1.15)	11.38 (13.65)

^a The first numbers are for an *S,SS* configuration of the catalyst, and the numbers in parentheses are for the *S,RR* configuration of the catalyst.

tively similar to the *S,SS* and *R,SS* forms of the system discussed here, are likely to coexist and interconvert rapidly compared to the time scale of catalysis. Finally, the *o,o'*-bis(diphenylphosphino)biphenyl (BIPHEP) ligand forms complexes with ruthenium analogous to the (BINAP)Ru(H)₂(diamine) catalyst, and enantioselectivity has been observed in ketone hydrogenation.⁷ The biphenyl moiety is only moderately configurationally stable and is otherwise very similar to the BINAP ligand. The dichloride precursor of the catalyst has been shown⁷ to exist in two slowly interconverting forms, similar to those of the *S,SS* and *R,SS* forms of the BINAP,cydn catalyst studied here computationally. This is almost certainly true for the dihydride catalyst also. In the three cases, therefore, species of similar relative energy and geometry to the *S,SS* and *S,RR* forms of the BINAP,cydn catalyst studied here computationally are expected to be present in equilibrium in solution and could contribute to catalysis.

As shown in Table 5, the *S,SS* form of the catalyst is predicted to lie very close in energy to the *S,RR* form. At the B3LYP/6-31G* and SCS-MP2/6-31G* levels of theory, the *S,RR* isomer is favored (by 0.40 and 0.11 kcal/mol, respectively), whereas with B3LYP and the larger basis, the preference is reversed, with the *S,SS* form favored by 1.28 kcal/mol. The small magnitude of the energy difference between these two isomers is easy to understand, as the cydn and BINAP ligands do not interact strongly, but the sign of this difference is hard to rationalize. The calculations do not help to resolve this latter question, as the levels of theory used here are not accurate enough to be converged with respect to this small energy difference. Nevertheless, it is reasonable to expect that for the systems mentioned above, which are able to undergo processes analogous to interconversion between the *S,SS* and *S,RR* isomers, solutions will contain mixtures of the two isomers and that both can contribute to catalysis.

Table 5 also enables one to compare the energies of all eight TSs that can in principle be accessed from catalysts in which interconversion can occur between isomers analogous to the *S,SS* and *S,RR* systems discussed. The lowest energy TS at all levels of theory is the ax-out TS derived from the *S,SS* catalyst already discussed above (+3.89 kcal/mol with B3LYP/6-31G*). This TS is favored by the axial orientation of the NH proton, the lack of steric hindrance between the acetophenone phenyl group, present in the lower right-hand quadrant of Figure 4, and the BINAP ligand, and the hydrogen bond with the phenyl ring. The identity of the second lowest energy TS depends on the level of theory. At the B3LYP/6-31G* level, it is the eq-out TS derived from the *S,RR* form of the catalyst (+5.25 kcal/mol), whereas at the B3LYP/6-311G** level, it is the ax-in TS derived from the more stable *S,SS* form of the catalyst.

Assuming that the energy difference between the two forms is approximately the same for the related systems mentioned above, what is the predicted outcome of hydrogenation based

on our calculations? For the (BINAP, en) system, ready interconversion of the two forms can occur, without change in chirality of the BINAP. The lowest TS will lead to *R* alcohol, as will the eq-out TS derived from the *S,RR* conformer of the catalyst. The lowest energy TS leading to *S* alcohol is the ax-in TS derived from the *S,SS* conformer. Hence, one might expect to obtain a somewhat similar value of the ee to that obtained with the full matched catalyst. Experimentally, the *R* product is indeed formed predominantly, but a significantly lower ee of only 57% is obtained, perhaps because the higher flexibility of the ethylenediamine ligand allows more structural relaxation in the ax-in TS.

For the ((PPh₃)₂, dpen) system, ready interconversion can occur between conformers corresponding to the *S,SS* form of the system studied here and the *R,SS* form. Again, as the ax-out TS derived from the *S,SS* is lowest in energy, preferential formation of *R* alcohol is expected. The next lowest-energy TS is the ax-in TS, and this leads to *S* alcohol. As in the previous case, one therefore expects a similar ee to that obtained with the fully chiral (BINAP, dpen) or (BINAP, cydn) systems. The lower ee obtained experimentally again suggests that in practice the array of two triphenyl phosphine ligands is more flexible than the BINAP ligand and can accommodate the ax-in TS more easily. It is also possible that the *R,SS* conformer can be formed, with reactivity occurring through the corresponding eq-out TS, which is second lowest in energy on the basis of the B3LYP/6-31G* calculations. This TS leads to the *S* enantiomer of the alcohol, so could explain the lower ee.

Although more precise predictions about the behavior of these mixed systems would ideally be derived from actual calculations, it is nevertheless encouraging that the present calculations already can be used to predict the sign of the enantioselectivity. This shows that stereoselectivity in reactions of many of the Ru(phosphine)₂(diamine) dihydride catalysts has a similar origin to that explored here in detail for the BINAP,cydn system. In particular, a fairly large number of successful catalysts have been developed in which the phosphine moiety or the diamine is not chiral, but enantioselectivity depends in part on the induction of a chiral environment by either the diamine or diprophine.⁴⁶

Conclusions

Understanding the origin of the asymmetric hydrogenation of ketones by RuH₂(diphosphine)(diamine) complexes is crucial to the development of new, more active, more selective, and/or more robust catalysts. Our calculations are in good agreement with experimental data concerning this reaction.⁴⁷ The study of the small model system (H₃P)₂RuH₂(en) shows that the key step for hydrogenation is simultaneous transfer of a hydride from ruthenium to carbon, and a proton from nitrogen to oxygen. This step occurs with a near-planar arrangement of the six atoms involved (HRuNH and CO). With 1,2-diamine chelating ligands, as are commonly used in this reaction, the NH₂ protons in the chelate ring adopt either pseudoaxial (H_{ax}) or pseudoequatorial (H_{eq}) geometries. In the model system, the hydrogenation transition state involving transfer of the H_{ax} proton is ca. 2 kcal/

(46) (a) See for example: Jing, Q.; Zhang, X.; Sun, J.; Ding, K. *Adv. Synth. Catal.* **2005**, *347*, 1193–1197. (b) Jing, Q.; Sandoval, C. A.; Wang, Z.; Ding, K. *Eur. J. Org. Chem.* **2006**, 3606–3616. (c) Xia, Y. Q.; Tang, Y. Y.; Liang, Z. M.; Yu, C. B.; Zhou, X. G.; Li, R. X.; Li, X. J. *J. Mol. Catal. A: Chem.* **2005**, *240*, 132–138.

(47) In fact, the prediction in our earlier work (ref 16) that hydrogen splitting was turnover limiting was made *before* experimental evidence for this became available.

mol lower in energy than that involving the H_{eq} proton, presumably because this enables the system to adopt a more favorable, less twisted geometry at the TS. Test calculations on the model system show that the level of theory used is reasonably well converged.

Calculations on the hydrogenation of a nonsymmetric ketone, acetophenone, by the same model catalyst show that the potential energy surface is very similar for this system. In this case, however, for both the reaction modes involving H_{ax} and H_{eq} transfer, the acetophenone moiety can approach the catalyst in two different orientations, with the phenyl group pointing *in* toward the phosphine ligands or *out*. We hence find four different TSs, with those involving H_{ax} transfer again being lower in energy than those involving H_{eq} transfer. The *out* TSs in which the phenyl group is oriented away from the phosphine groups are also slightly lower than the corresponding *in* TSs, either due to steric repulsion between the phenyl groups and the phosphine ligands in the *in* TSs or due to stabilizing hydrogen bonds between the phenyl group and the metal-coordinated NH₂ group in the *out* TS.

Calculations on the “real” (BINAP)RuH₂(cydn) catalyst, in both its matched *S,S* and mismatched *S,RR* forms, reproduce the observed experimental selectivities in a semiquantitative way. The basic features of the potential energy surfaces in these reactions are similar to those obtained for the model system, validating use of the latter in previous work. Test calculations again show that the main B3LYP/6-31G* level of theory used to study the reaction is of adequate accuracy. Analysis of the structure of the key hydrogenation TSs helps to rationalize the selectivity, based on three key factors: steric interactions between the bulkier of the two ketone substituents and the BINAP ligand, differential intrinsic reactivity of the H_{ax} and H_{eq} protons on the diamine ligand, and hydrogen bonding between the diamine NH₂ group and the phenyl group on the ketone. In this matched system, all of these factors are favorable for the lowest, ax-out TS, and this explains the observed *R* selectivity. The second lowest TS is the ax-in TS, in which the hydrogen bond is lost and steric factors are less favorable. The possible importance of the hydrogen bonding is emphasized by the fact that dialkyl ketones tend to give lower enantioselectivities.⁸

For the mismatched system, none of the located TSs are favorable with respect to all three of the factors mentioned above. Hence the lowest energy eq-out TS, which is favored

by steric effects and hydrogen bonding, and the next lowest, the ax-out TS, which benefits from the better intrinsic reactivity of the H_{ax} proton, are quite close in energy. This accounts for the lower selectivity. We note that the fact that *R* alcohol is favored with the mismatched catalyst cannot be explained without considering the possibility of involvement of the a priori less reactive H_{eq} proton.

Although our computational study considers only one catalyst system, (BINAP)RuH₂(cydn), it yields insight into the selectivity observed with many other catalysts. For example, the greater steric bulk in the XylBINAP ligand tends to lead to higher selectivities. The geometry of the 1,2-diphenylethylenediamine ligand (dpn) in complexes with ruthenium dihydrides is very similar to that of the 1,2-cyclohexanediamine (cydn) ligand studied here. Both are known to lead to similar stereoselectivity. Our study was conducted using cydn for reasons of computational efficiency, but the results should be applicable to the dpn complexes also. As noted above, the fact that dialkylketones cannot be hydrogenated with high enantioselectivities in such a straightforward way as alkyl aryl ketones is also rationalized by our results, in terms of the absence of a stabilizing hydrogen bond interaction. Finally, our results on the conformationally rigid (BINAP)RuH₂(cydn) system can be extrapolated to make predictions for the stereochemically less well defined (biphep)RuH₂(dpn), (Ph₃P)₂RuH₂(dpn), and (BINAP)RuH₂(en). Our calculations predict the sign of the enantioselectivity correctly for all of these systems.

Acknowledgment. The authors are indebted to the Belgian National Fund for Scientific Research (FNRS) for its financial support to this research (T.L. is a Postdoctoral Researcher). They would also like to thank the FNRS for its support to access a computational facilities project (project no. 2.4502.05). J.N.H. thanks the EPSRC for an Advanced Research Fellowship. We would also like to acknowledge useful discussions with Natalie Fey and Bob Morris.

Supporting Information Available: B3LYP/6-31G*-optimized cartesian coordinates for all species. This material is available free of charge via the Internet at <http://pubs.acs.org>.

OM700940M